Streptococcus pneumoniae induces expression of the antibacterial CXC chemokine MIG/CXCL9 via MyD88-dependent signaling in a murine model of airway infection.

Eliasson, Mette; Mörgelin, Matthias; Farber, Joshua M; Egesten, Arne; Albiger, Barbara

Published in:
Microbes and Infection

DOI:
10.1016/j.micinf.2010.03.014

2010

Document Version:
Peer reviewed version (aka post-print)

Streptococcus pneumoniae induces expression of the antibacterial CXC chemokine MIG/CXCL9 *via* MyD88-dependent signaling in a murine model of airway infection

Mette Eliasson[a], Mathias Mörgelin[b], Joshua M. Farber[d], Arne Egesten[a], Barbara Albiger[e*]

Lund University and Lund University Hospital, Department of Clinical Sciences,
[a] Section for Respiratory Medicine, and Allergology [b]Clinical and Experimental Infection Medicine, [e] Dermatology and Venerology, 221 84 Lund, Sweden.

[d] National Institute of Health, National Institute of Allergy and Infectious Diseases, Laboratory of Molecular Immunology, Bethesda, USA.

*Corresponding author:
Barbara Albiger, PhD
Lund University and Lund University Hospital
Biomedical Center,
Department of Clinical Sciences
Division of Dermatology and venerology
Tornavägen 10
SE-221 84 Lund
Sweden
Tel: 00 46 (0)46 222 30 63
Fax: 00 46 (0)46 15 77 56

Abstract (148 words):

MIG/CXCL9 belongs to the CXC family of chemokines and participates in the regulation of leukocyte trafficking and angiogenesis. Certain chemokines, including human MIG/CXCL9, exerts strong antibacterial activity *in vitro*, although the importance of this property *in vivo* is unknown. In the present study, we investigated the expression and a possible role for MIG/CXCL9 in host defence during mucosal airway infection caused by *Streptococcus pneumoniae in vivo.* We found that intranasal challenge of C57BL/6 wild-type mice with pneumococci elicited production of high levels of MIG/CXCL9 in the lungs *via* the MyD88-dependent signaling pathway. Whereas both human and murine MIG/CXCL9 showed efficient killing of *Streptococcus pneumoniae in vitro*, MIG/CXCL9 knockout mice were not more susceptible to pneumococcal infection. Our data demonstrate that, *in vivo* this chemokine probably has a redundant role, acting together with other antibacterial peptides and chemokines, in innate and adaptive host defense mechanisms against pneumococcal infections.

Key words: Gram-positive bacteria; *Streptococcus pneumoniae*; Innate immunity; Antimicrobial chemokines; Toll-Like Receptors; Epithelial cells.

Abbreviations: TLRs, Toll-like receptors; IFN, interferon; LTA, lipotechoic acid; Cfu, colony forming units; wt, wild-type KO, knock out; NAL, nasopharyngeal lavage; p.i., post infection; i.n., intranasal; Human primary bronchial epithelial cells, HBEC;

1. Introduction

Streptococcus pneumoniae (the pneumococcus) is an encapsulated Gram-positive bacterium with ninety-one different capsules or serotypes identified so far. This bacterium is a common colonizer of the nasopharynx in children, but can also cause life-threatening diseases such as pneumonia and invasive pneumococcal diseases (i.e. sepsis and meningitis), killing more than 2 millions people in the world every year and leaving severe sequelae in many children [1].

The Toll-Like Receptors (TLRs) play an important role in host defense against microbial infections including pneumococci [2]. They recognize conserved bacterial structures or also called pathogen-associated molecular patterns (PAMPs). Upon recognition of their cognate ligands, TLRs can initiate two distinct signaling cascades, the MyD88-dependent or the MyD88-independent, leading to either the production of proinflammatory cytokines or the production of type I interferons (IFNs) [2]. Pneumococci express several PAMPs such as lipoteichoic acids (LTA), pneumolysin, and hypomethylated DNA containing CpG motifs that are ligands for TLR2, TLR4 and TLR9 respectively [3-5]. Recent studies showed that mice deficient in TLR2 are only marginally affected in their susceptibility to invasive pneumococcal disease, while both TLR4 and TLR9 play important roles in controlling pneumococcal colonization and the early clearance of bacteria from the lower respiratory tract. We have shown that MyD88-deficiency in mice results in uncontrolled bacterial growth in the airways leading to rapid bacterial dissemination into the bloodstream resulting in systemic infection [4]. The increased susceptibility of MyD88-deficient mice is illustrated by an impaired local production of proinflammatory cytokines and chemokines [4].

Chemokines is a large family of peptides unified by their ability to exert receptor-

dependent regulation of leukocyte-trafficking during both health and disease [6]. They are divided into four groups, C, CC, CXC, and CX_3C respectively, depending on the arrangement of conserved cysteine-motifs in their NH_2-terminal region. In addition to their interactions with leukocytes, chemokines regulate other events during inflammation, for example angiogenesis and angiostasis, and yet some have potent antibacterial activity themselves [7]**.** The monokine induced by IFN-γ, MIG/CXCL9 belongs to the CXC chemokine family and is expressed by epithelial cells and granulocytes during Th_1-polarized inflammation [8]. It exhibits strong antibacterial activity *in vitro* against several pathogens [9, 10]. Recently, we found MIG/CXCL9-dependent antibacterial activity against *S. pyogenes* at the surface of IFN-γ stimulated pharyngeal epithelial cells *in vitro* [9]. This led us to investigate the expression and a possible role for MIG/CXCL9 *in vivo* during mucosal airway infection caused by *Streptococcus pneumoniae.*

In this study, two murine models of pneumococcal pneumonia (non-lethal resolving and acute pneumonia) were used to investigate potential key roles for MIG/CXCL9 in host defense functions. We show that MIG/CXCL9 is expressed in the lungs upon pneumococcal infection in a MyD88-dependent manner. We also demonstrate that *in vitro* MIG/CXCL9 has antibacterial activity against *S. pneumoniae.* However, we were unable to demonstrate that MIG/CXCL9 is essential for microbial clearance and host survival *in vivo*.

2. Materials and methods

2.1 Bacterial strain and culture conditions

Streptococcus pneumoniae TIGR4 is a clinical encapsulated isolate of serotype 4 (ATCC BAA-334; http://www.tigr.org). For *in vitro* experiments, bacteria were grown overnight from frozen stocks on blood agar plates at 37°C and 5% CO_2. Colonies were grown in TH (Todd-Hewitt) broth supplemented with 0.5% yeast extract to OD_{600nm}=0.4-0.5. Appropriate dilutions were made to obtain the desired concentration. The concentrations were retrospectively confirmed by counting colony-forming units (cfu) on blood agar plates.

2.2 Mice and infection models

C57BL/6 (wt), ICE-, TLR4-, TLR9- and MIG/CXCL9-deficient mice (six to eight weeks old) were kept under pathogen-free conditions. The ICE knock-out (KO) mice are unable to release functional IL-1 and IL-18. All KO mice had been backcrossed for at least seven generations on the C57BL/6 background. The animals were housed five per cage in a standardized 12 h light/dark cycle and received commercial food and water *ad libitum*. All the experiments were conducted in conformity with the European Communities Council Directive 86/609/EEC and the Swedish Animal Protection Legislation. All animal groups were age and sex matched for each experiments. For the non-lethal resolving pneumonia model, mice were inoculated intranasally (i.n.) with vehicle (PBS) or TIGR4 (10^5 cfu/mouse) in a volume of 20 µl. For the acute pneumonia/bacteremia model, mice were infected i.n. with vehicle (PBS) or TIGR4 (10^7cfu/mouse). The health status and survival of the mice, including sampling from blood, lungs and nasopharyngeal-tracheal lavages (NAL) were performed as previously described [4]. Briefly, to evaluate bacteremia,

blood samples (5 μl) were obtained from the tail vein at various time-points and used for serial plating to quantify viable bacteria by cfu. The lungs were removed and homogenized in 1 ml of PBS containing a complete cocktail protease inhibitor (Roche Diagnostics Scandinavia) and used in serial dilutions to quantify viable bacteria by plating on blood agar plates. The homogenates were centrifuged at 4°C for 30 min at 5000 rpm and the supernatants were stored at -80°C for later cytokine and chemokine analysis. NAL were performed in animals post-mortem with a 20-gauge catheter inserted into the proximal trachea, flushing the nasopharynx through the trachea and the nares with 200 μl PBS and used in serial plating to quantify viable bacteria.

2.3. Proteins and antibodies

Recombinant human and murine MIG/CXCL9 were purchased from Peprotech, Rocky Hill, NJ. The polyclonal goat antibody against MIG/CXCL9, the goat isotype control, human and murine TNF-α as well as human and murine IFN-γ were obtained from R&D Systems, Abingdon, UK.

2.4. *In vitro* killing assays

2.4.1. Bronchial epithelial killing

Human primary bronchial epithelial cells (HBEC) were obtained from Lonza Copenhagen. HBEC were seeded in 24-well tissue culture plates and cultured to confluence (1 x 10^6cells/well) in MEM supplemented with 10% heat-inactivated fetal bovine serum and penicillin/streptomycin (100 U/ml and 0.1 ng/ml respectively) at 37°C in an atmosphere containing 5% CO_2 with 100% relative humidity. HBEC were washed with MEM and then incubated in medium alone (control) or stimulated with

IFN-γ (10 ng/ml), TNF-α (10 ng/ml) or IFN-γ (10 ng/ml) + TNF-α (10 ng/ml) for 24 h. Subsequently, 50 µl of bacteria (TIGR4; $2x10^6$/ml in incubation buffer; MOI=0.1) was layered on top of the epithelial cells. This was followed by centrifugation at 300 x g for 10 minutes to promote cell-bacteria interaction and incubation for 1 h at 37°C. Trypsin (2.5 mg/ml in PBS) was used to detach the cells from the wells and Triton X-100 (0.025% in PBS) was added to lyse the cells and release internalized bacteria. Bacterial killing was determined by viable counts after plating on blood agar plates.

2.4.2. MIG/CXCL9 killing

S. pneumoniae strain TIGR4 was grown to mid–logarithmic phase (OD_{620nm} = 0.4-0.5) in TH broth supplemented with 0.5 % yeast extract, washed, and diluted in 10 mM Tris (pH 7.5) containing 5 mM glucose (incubation buffer) to a concentration of 1%. Fifty microliters of bacteria (2 x 10^6 cfu/ml) were incubated with human or murine MIG/CXCL9 at different concentration or in buffer alone for 2 h at 37°C. To quantitate bactericidal activity, serial dilutions of the incubation mixtures were plated on blood agar plates, and the number of cfu was determined.

2.5. Stimulation of human and murine bronchial epithelial cells

MLE-12, a murine bronchial epithelial cell line (a gift from Dr. Jeffrey Whitsett, Children's Hospital Medical Center, Cincinnati, USA) was cultured to semi confluent layers in DMEM+GlutaMAX supplemented with 10% heat-inactivated fetal bovine serum and penicillin/streptomycin (100 U/ml and 0.1 ng/ml respectively) at 37°C in an atmosphere containing 5% CO_2 with 100 % relative humidity. HBEC were seeded in 24-well tissue culture plates and cultured to confluence. Cells were stimulated in 24-well plates for 24 h as follows: culture medium (control), IFN-γ (10 ng/ml), TNF-α

(10 ng/ml) and IFN-γ (10 ng/ml) + TNF-α (10 ng/ml). The supernatants were collected and the MIG/CXCL9 concentration was quantified using ELISA.

2.6. Determination of cytokine and chemokine levels

TNF-α, IFN-γ and MIG/CXCL9 of lung homogenates were measured using commercial ELISA kits (R&D Systems, Abingdon, UK). According to the manufacturer, the ELISAs are specific and do not recognize related peptides. The detection limit for the ELISA was set to 30 pg/ml and the samples were diluted so that values could be calculated from the linear part of the standard curves.

2.7. Modeling a predictive structure of murine and human MIG/CXCL9

2.7.1. Sequence alignment

The pairwise sequence comparison and alignment between mouse and human CXCL9 were generated using ClustalW [11].

2.7.2 Molecular modeling

Model structures of full length human and mouse MIG/CXCL9 (accession number Q07325 and P18340, respectively) were generated as comparative homology models using the NMR structure of truncated human MIP2-α (Gro-β) with Protein Data Bank code 1QNK as template [12]. Residues 23-125 of human MIG/CXCL9 were aligned against the sequence of MIP2-α creating an alignment where MIP2- α residues 39-107 matched to human MIG/CXCL9 residues 27-96 with only one gap at threonine 40 of human MIG/CXCL9. The sequence identity was 49 %. The modeling was performed using the program MODELLER version 9v7 [13-15]. Ten models were generated using the automodel class and the model with the lowest DOPE assessment score were selected. The NH_2- and COOH-terminal parts of human

MIG/CXCL9 (residues 23-26 and 97-125, respectively) lack template and were thus modeled in an extended conformation. Human and mouse MIG/CXCL9 are very similar in sequence with an identity of 68 %. Hence, the model of mouse MIG/CXCL9 was generated in a similar manner. Residues 22-126 were aligned to the template with MIP2-α residues 39-107 matching residues 26-95 of mouse MIG/CXCL9 with a gap at threonine 39 of mouse CXCL9. Molecular representations of the models were made using PyMOL [16].

2.8. Imaging techniques

2.8.1. Histology

Tissues were fixed in 4% paraformaldehyde, embedded in paraffin and cut to a thickness of 4 µm. Deparaffinized tissue sections were incubated with polyclonal goat antibodies against MIG/CXCL9 or goat isotype control antibody at a final concentration of 5 µg/ml. The staining procedure was performed using a DAKO TechMate 500/1000 Instrument and the manufacturer's detection kit (DAKO ChemMate Detection Kit Peroxidase/DAB). The sections were weakly counterstained with Mayer's hematoxylin solution.

2.8.2. Negative staining and transmission electron microscopy

Bacteria were incubated for 2 h at 37°C in incubation buffer, in the absence or presence of MIG/CXCL9 (2.4 µg/ml). Negative staining of the bacteria was performed with 0.75% uranyl formate. Specimens were examined in a Jeol 1200 EX transmission electron microscope operated at 60 kV accelerating voltage.

2.9. Statistical evaluation

Significant differences were evaluated using the Student's *t* test. The survival was analyzed by Kaplan-Meier log rank test.

3. Results

3.1 IFN-γ stimulated human bronchial epithelial cells are bactericidal

Human bronchial epithelial cells (HBEC) express high levels of MIG/CXCL9 in response to IFN-γ stimulation [8]. We confirmed that HBEC produce high levels of MIG/CXCL9 in response to IFN-γ, but not in response to TNF-α stimulation. Moreover, a twofold increase in MIG/CXCL9 production was observed when IFN-γ and TNF-α were combined, highlighting a synergistic effect of IFN-γ and TNF-α on MIG/CXCL9 expression (Fig.1A). After stimulation with IFN-γ and TNF-α and IFN-γ combined, but not with TNF-α alone, HBEC also exhibited antibacterial activity as compared to non-stimulated control cells (Fig.1B). The antibacterial activity of HBEC correlated with high levels of MIG/CXCL9 production suggesting a direct causality between MIG/CXCL9 production and the antibacterial activity. Controls experiments showed that neither IFN-γ nor TNF-α themselves or combined have any antimicrobial activity *per se* (data not shown).

Taken together, our data demonstrate that during an inflammatory state, HBEC are antibacterial against *S. pneumoniae*, possibly through the production of MIG/CXCL9.

3.2. Human and murine MIG/CXCL9 kill *Streptococcus pneumoniae* efficiently *in vitro*

To test whether MIG/CXCL9 is antibacterial against *S. pneumoniae*, we performed *in vitro* killing assays. Human MIG/CXCL9 displayed a strong and dose-dependent antibacterial activity against *S. pneumoniae* TIGR4 strain (Fig. 2A), which can be blocked with a polyclonal anti-MIG/CXL9 antibody (data not shown). Investigation of bacterial morphology using electron microscopy and negative staining showed that MIG/CXCL9 exposure caused lysis and leakage of intracellular content (Fig. 2B).

Sequence alignments showed that human and murine MIG/CXCL9 are highly conserved with an overall of 67 % identity and 80 % similarity on the amino acid level (Fig. 2C). Structural prediction revealed that both molecules have a similar three-dimensional structure consisting of three anti-parallel β-sheets and amphipatic α-helix with unordered tail regions (Fig. 2D). Recombinant murine MIG/CXCL9 showed a potent antibacterial activity against TIGR4 (Fig. 2A), demonstrating that the antibacterial function is conserved between the murine and human molecules.

3.4. Cytokine-stimulated murine bronchial epithelial cells express high levels of MIG/CXCL9

Murine lung epithelial cells (MLE-12) produced high levels of MIG/CXCL9 in response to IFN-γ, but not TNF-α stimulation. A 10-fold increase in MIG/CXCL9 production was observed when IFN-γ and TNF-α were combined (Fig. 3) demonstrating the same synergistic effect of IFN-γ and TNF-α on MIG/CXCL9 expression as described above for the HBEC. Our data confirm that inflamed murine bronchial epithelial cells are capable of producing MIG/CXCL9.

3.5. MIG/CXCL9 is produced in the lungs during pneumococcal pneumonia

Wild-type (wt) mice were infected intranasally (i.n.) with TIGR4 strain. We found that TNF-α, IFN-γ and MIG/CXCL9 were expressed in the lungs during infection *in vivo*. Both TNF-α and IFN- γ expression was maximal at 12 h post infection (pi) and remained stable up to 24 h pi, while MIG/CXCL9 expression peaked 24 h after inoculation; a sequential expression confirming that IFN-γ and TNF-α production precede that of MIG/CXCL9 (Fig. 4A). Histopathological examination and immunohistochemistry staining showed the presence of professional immune cells

into the lung tissue and the local production of MIG/CXCL9 in the airways during infection (Fig. 4B). Thus, TNF-α, IFN-γ and MIG/CXCL9 are expressed in the lungs upon pneumococcal infection, suggesting important roles of these proinflammatory mediators in host protection.

3.6. MyD88-signalling is required for MIG/CXCL9 production in the lungs

The central adaptor MyD88 of the TLRs signaling has a key role during pneumococcal pneumonia [3, 4]. Upon pneumococcal challenge, the local expression of IL-12 but not IFN-γ was dependent on the MyD88 signaling pathway (Fig. 5A and 5B). Next, we investigated the contribution of MyD88 and TLRs signaling in pneumococci-induced MIG/CXCL9 expression. MyD88 KO mice showed significantly lower levels of MIG/CXCL9 in the lungs as compared with wt mice (Fig. 5C). We found no significant difference in MIG/CXCL9 production in the lungs of the single TLRs KO (Fig. 5C). Taken together, our data show that MIG/CXCL9 production in the lungs upon pneumococcal challenge is dependent mainly on the MyD88 signaling pathway.

3.7. MIG/CXCL9 is not essential for survival in airway infection caused by *Streptococcus pneumoniae*

To study the mucosal antibacterial function of MIG/CXCL9 *in vivo*, we infected wt and MIG/CXCL9 KO mice i.n. with a low infectious dose of TIGR4 (10^5 cfu), which leads to a non-lethal resolving pneumonia and colonization up to 15 days [3]. No difference in survival or nasopharyngeal colonization was observed between wt and KO mice (Fig. 6). In an acute pneumonia model, wt and MIG/CXCL9 KO mice were infected i.n. with a high infectious dose of TIGR4 (10^7 cfu). In this model, the bacteria

can disseminate from the lungs to the bloodstream and the animal succumbs to an overwhelming systemic infection. The survival of the mice in the two groups was almost identical over time following initiation of the infection (Fig. 6). Bacterial loads in the blood, in the NAL and in the lungs were equivalent in both groups (data not shown). Thus, the absence of MIG/CXCL9 does not affect clearance of pneumococci from the upper and lower respiratory tract or susceptibility to invasive infection in a murine model of *S. pneumoniae* infection.

4. Discussion

In this work, we investigated the expression and the possible importance for MIG/CXCL9 in mucosal host defense during respiratory infections caused by *S. pneumoniae.*

The respiratory epithelium is continuously exposed to inhaled particles and pathogens. It is an important source of mediators of lung inflammation such as chemokines, which are crucial for the recruitment of leukocytes into sites of infection. Therefore, they constitute an important first line of defense against airborne infections [17]. Human bronchial epithelial cells (HBEC) express high levels of MIG/CXCL9 in response to IFN-γ stimulation [8]. We showed that primary HBEC stimulated with IFN-γ exhibit antibacterial activity against *S. pneumoniae*. Furthermore, during pneumococcal infection, IFN-γ and MIG/CXCL9 are expressed in the lungs of wt mice, suggesting potential key roles of these inflammatory mediators in host defense.

The sequence and the predicted three-dimensional structure of murine and human MIG/CXCL9 are highly conserved. *In vitro*, both human and murine MIG/CXCL9 kill pneumococci efficiently, demonstrating that the antibacterial activity is also conserved and may be an important feature of this molecule.

Even though MIG/CXCL9 expression is critically dependent on IFN- γ and the interferon-dependent transcription factor, STAT1, the MIG/CXCL9 gene contains NF-kB responsive elements and its transcription is enhanced by a synergistic interaction between STAT1 and NF-kB [18, 19]. We could confirm *in vitro* that TNF-α synergizes with IFN-γ to induce production of MIG/CXCL9 by bronchial epithelial cells. *In vivo*, the local production of IL-12 but not IFN-γ is impaired in the MyD88-deficient mice,

which led us to hypothesize that the expression of MIG/CXCL9 might be dependent of the MyD88-signaling. Indeed, MIG/CXCL9 expression is reduced in MyD88 KO mice. Thus, our results in MyD88 KO mice emphasize the importance of the enhancement of MIG/CXL9 expression *via* TLR/IL-1R-dependent activation of the NF-kB pathway. MyD88 is also involved in the IL-1/IL-18 R signaling but we excluded a possible role for IL-1/IL-18 as mediators for MIG/CXCL9 production since ICE KO mice express high amounts of MIG/CXCL9 (data not shown). However, the MIG/CXCL9 expression is not blunted in TLR4 and TLR9 KO mice, suggesting either redundancy between the TLRs or the involvement of a yet unidentified non-redundant MyD88-dependent receptor. Recently, it was demonstrated that Group A streptococci induce cytokines and chemokines production in a MyD88-dependent manner without the involvement of TLR2, TLR4 and TLR9 and that Group B streptococci induce type I IFN production *via* TLR7-dependent, MyD88-dependent signaling [20-22].

However, murine MIG/CXCL9 did not decrease bacterial dissemination or colonization and MIG/CXCL9 KO mice are not more susceptible to infection than wt animals. We do not know, whether the levels of MIG/CXCL9 found in tissue homogenates are bactericidal, how these molecules are exposed and whether they can exert antibacterial activity *in vivo*. One plausible explanation is that *in vivo* this chemokine have a redundant role, acting together with other antibacterial peptides and chemokines, in innate and adaptive host defense mechanisms counteracting bacterial infections. There are two closely related chemokines that belong to the CXC family, IP-10/CXCL10 and I-TAC/CXCL11 respectively. They share the ability with MIG/CXCL9 to signal through CXC chemokine receptor 3 (CXCR3). They also exhibit antibacterial activity *in vitro* and might compensate for the absence of

MIG/CXCL9 *in vivo*. In a murine model of *Klebsiella pneumoniae* pneumonia, IP-10/CXCL10 but not MIG/CXCL9 promoted Type 1 immunity [23]. Infection of CXCR3 KO mice with the pneumococcal TIGR4 strain showed a higher colonization level in the nasopharynx of CXCR3 KO as compared to wild type animals despite no significant difference in survival (data not shown). A persistent colonization might lead to the development of invasive disease. Another indication of redundancy is that recent Genbank submissions revealed a single bp deletion in the coding sequence (13th codon) for I-TAC/CXCL11, a gene close to MIG/CXCL9 and IP-10/CXCL10 on mouse chromosome 5 of the C57BL/6 mice. The C57BL/6 I-TAC/CXCL11 sequence is predicted to produce a truncated, non-functional protein. The GenBank sequence of I-TAC/CXCL11 in the 129sv strain has an I-TAC/CXCL11 ORF without the deletion. Because the MIG/CXCL9 gene was targeted in ES cells from the 129sv strain, and because of the close linkage of MIG/CXCL9 and I-TAC/CXCL11, we have sequenced the relevant I-TAC/CXCL11 sequences in our wt and MIG/CXCL9 KO mice and we found out that the MIG/CXCL9 KO mice have the 129sv strain sequence for I-TAC/CXCL11, predicted to encode a full length I-TAC/CXCL11. One consequence might be that because MIG/CXCL9, IP-10/CXCL10 and I-TAC/CXCL11 share CXCR3, a functional I-TAC/CXCL11 in the MIG/CXCL9 KO mice underestimates the effects of knocking out MIG/CXCL9 in experimental comparisons with the C57BL/6 wt mice. The potential roles of IP-10/CXCL10 and I-TAC/CXCL11 in pneumococcal infections are under investigation.

MIG/CXCL9 is also a chemaoattractant for T cells and NK cells to inflammatory sites where IFN-γ is produced. Thus, we cannot exclude a role of MIG/CXCL9 in recruiting CD4+ T cells to the site of infection. Clearance of pneumococci is dependent upon the rapid recruitment and presence of CD4+ T cells at the time of infection

suggesting a previously underestimated role for the cellular players of the adaptive immune system in the control and clearance of this pathogen [24, 25].

In conclusion, we could identify an antimicrobial role for MIG/CXCL9 *in vitro* but not *in vivo,* most likely explained by an important redundancy among key molecules regulating host defense.

6. Acknowledgements

We would like to thank Elise Nilsson for technical assistance with the histology. BA, AE and ME were supported by grants from the Swedish Medical Research Council, the Swedish Heart and Lung Foundation, the Swedish Society of Medicine, the Medical Faculty at Lund University and the Foundations of Crafoord, Bergh, Ihre, Hedberg, Kock, Marcus & Marianne Wallenberg, Lars Hiertas, Alfred Österlund, Längmanska and OE & Edda Johansson.

References

[1] K.L. O'Brien, L.J. Wolfson, J.P. Watt, E. Henkle, M. Deloria-Knoll, N. McCall, E. Lee, K. Mulholland, O.S. Levine, T. Cherian, Burden of disease caused by Streptococcus pneumoniae in children younger than 5 years: global estimates, Lancet 374 (2009) 893-902.

[2] B. Albiger, S. Dahlberg, B. Henriques-Normark, S. Normark, Role of the innate immune system in host defence against bacterial infections: focus on the Toll-like receptors, J Intern Med 261 (2007) 511-528.

[3] B. Albiger, S. Dahlberg, A. Sandgren, F. Wartha, K. Beiter, H. Katsuragi, S. Akira, S. Normark, B. Henriques-Normark, Toll-like receptor 9 acts at an early stage in host defence against pneumococcal infection, Cell Microbiol 9 (2007) 633-644.

[4] B. Albiger, A. Sandgren, H. Katsuragi, U. Meyer-Hoffert, K. Beiter, F. Wartha, M. Hornef, S. Normark, B.H. Normark, Myeloid differentiation factor 88-dependent signalling controls bacterial growth during colonization and systemic pneumococcal disease in mice, Cell Microbiol 7 (2005) 1603-1615.

[5] R. Malley, P. Henneke, S.C. Morse, M.J. Cieslewicz, M. Lipsitch, C.M. Thompson, E. Kurt-Jones, J.C. Paton, M.R. Wessels, D.T. Golenbock, Recognition of pneumolysin by Toll-like receptor 4 confers resistance to pneumococcal infection, Proc Natl Acad Sci U S A 100 (2003) 1966-1971.

[6] A. Viola, A.D. Luster, Chemokines and their receptors: drug targets in immunity and inflammation, Annu Rev Pharmacol Toxicol 48 (2008) 171-197.

[7] M. Eliasson, A. Egesten, Antibacterial chemokines--actors in both innate and adaptive immunity, Contrib Microbiol 15 (2008) 101-117.

[8] A. Sauty, M. Dziejman, R.A. Taha, A.S. Iarossi, K. Neote, E.A. Garcia-Zepeda, Q. Hamid, A.D. Luster, The T cell-specific CXC chemokines IP-10, Mig, and I-TAC are expressed by activated human bronchial epithelial cells, J Immunol 162 (1999) 3549-3558.

[9] A. Egesten, M. Eliasson, H.M. Johansson, A.I. Olin, M. Morgelin, A. Mueller, J.E. Pease, I.M. Frick, L. Bjorck, The CXC chemokine MIG/CXCL9 is important in innate immunity against Streptococcus pyogenes, J Infect Dis 195 (2007) 684-693.

[10] H.M. Linge, I. Sastalla, D.P. Nitsche-Schmitz, A. Egesten, I.M. Frick, Protein FOG is a moderate inducer of MIG/CXCL9, and group G streptococci are more tolerant than group A streptococci to this chemokine's antibacterial effect, Microbiology 153 (2007) 3800-3808.

[11] J.D. Thompson, D.G. Higgins, T.J. Gibson, CLUSTAL W: improving the sensitivity of progressive multiple sequence alignment through sequence weighting, position-specific gap penalties and weight matrix choice, Nucleic Acids Res 22 (1994) 4673-4680.

[12] Y.Q. Qian, K.O. Johanson, P. McDevitt, Nuclear magnetic resonance solution structure of truncated human GRObeta [5-73] and its structural comparison with CXC chemokine family members GROalpha and IL-8, J Mol Biol 294 (1999) 1065-1072.

[13] N. Eswar, B. John, N. Mirkovic, A. Fiser, V.A. Ilyin, U. Pieper, A.C. Stuart, M.A. Marti-Renom, M.S. Madhusudhan, B. Yerkovich, A. Sali, Tools for comparative protein structure modeling and analysis, Nucleic Acids Res 31 (2003) 3375-3380.

[14] N. Eswar, B. Webb, M.A. Marti-Renom, M.S. Madhusudhan, D. Eramian, M.Y. Shen, U. Pieper, A. Sali, Comparative protein structure modeling using Modeller, Curr Protoc Bioinformatics Chapter 5 (2006) Unit 5 6.
[15] N. Eswar, B. Webb, M.A. Marti-Renom, M.S. Madhusudhan, D. Eramian, M.Y. Shen, U. Pieper, A. Sali, Comparative protein structure modeling using MODELLER, Curr Protoc Protein Sci Chapter 2 (2007) Unit 2 9.
[16] W.L. DeLano, The PyMOL Molecular Graphics System, DeLano Scientific, San Carlos, CA. , (2002).
[17] K.S. Tsai, M.H. Grayson, Pulmonary defense mechanisms against pneumonia and sepsis, Curr Opin Pulm Med 14 (2008) 260-265.
[18] S. Mahalingam, G. Chaudhri, C.L. Tan, A. John, P.S. Foster, G. Karupiah, Transcription of the interferon gamma (IFN-gamma)-inducible chemokine Mig in IFN-gamma-deficient mice, J Biol Chem 276 (2001) 7568-7574.
[19] Y. Ohmori, R.D. Schreiber, T.A. Hamilton, Synergy between interferon-gamma and tumor necrosis factor-alpha in transcriptional activation is mediated by cooperation between signal transducer and activator of transcription 1 and nuclear factor kappaB, J Biol Chem 272 (1997) 14899-14907.
[20] N. Gratz, M. Siller, B. Schaljo, Z.A. Pirzada, I. Gattermeier, I. Vojtek, C.J. Kirschning, H. Wagner, S. Akira, E. Charpentier, P. Kovarik, Group A streptococcus activates type I interferon production and MyD88-dependent signaling without involvement of TLR2, TLR4, and TLR9, J Biol Chem 283 (2008) 19879-19887.
[21] G. Mancuso, M. Gambuzza, A. Midiri, C. Biondo, S. Papasergi, S. Akira, G. Teti, C. Beninati, Bacterial recognition by TLR7 in the lysosomes of conventional dendritic cells, Nat Immunol 10 (2009) 587-594.
[22] M. Liljeroos, R. Vuolteenaho, S. Rounioja, B. Henriques-Normark, M. Hallman, M. Ojaniemi, Bacterial ligand of TLR2 signals Stat activation via induction of IRF1/2 and interferon-alpha production, Cell Signal 20 (2008) 1873-1881.
[23] X. Zeng, T.A. Moore, M.W. Newstead, J.C. Deng, S.L. Kunkel, A.D. Luster, T.J. Standiford, Interferon-inducible protein 10, but not monokine induced by gamma interferon, promotes protective type 1 immunity in murine Klebsiella pneumoniae pneumonia, Infect Immun 73 (2005) 8226-8236.
[24] K. Trzcinski, C.M. Thompson, A. Srivastava, A. Basset, R. Malley, M. Lipsitch, Protection against nasopharyngeal colonization by Streptococcus pneumoniae is mediated by antigen-specific CD4+ T cells, Infect Immun 76 (2008) 2678-2684.
[25] R. Malley, K. Trzcinski, A. Srivastava, C.M. Thompson, P.W. Anderson, M. Lipsitch, CD4+ T cells mediate antibody-independent acquired immunity to pneumococcal colonization, Proc Natl Acad Sci U S A 102 (2005) 4848-4853.

Figure Legends:

Figure 1: Inflamed human bronchial epithelial cells exhibit antibacterial activity against *S. pneumoniae.*

A. Human primary bronchial epithelial cells (HBEC) were stimulated with TNF-α (10 ng/ml) or IFN-γ (10 ng/ml) alone or in combination for 24 h. Supernatant from cells stimulated with culture medium was used as a control. Supernatants were collected and the MIG/CXCL9 concentrations were quantified using ELISA. The data shown represent mean ±SEM. Data were analyzed by Student *t*-test. *, P<.05; **, P<.01; ***, P<.005

B. Unstimulated or stimulated human primary bronchial epithelial cells (HBEC) were infected with *S. pneumoniae* TIGR4 for 2 h at a MOI of 0.1 (equivalent to 1 x 10^5 cfu). The bactericidal activity was calculated by viable counts. The data shown represent the mean values of at least three independent experiments

Figure 2: Human and murine MIG/CXCL9 are conserved and kill pneumococci efficiently *in vitro*.

A. Bactericidal activity of human (circle) and murine MIG/CXCL9 (square) respectively against the invasive *Streptococcus pneumoniae* strain (TIGR4). Bacteria (2 x 10^6 cfu/ml) were incubated with increasing amounts of either human or murine MIG/CXCL9 (0.12-12 μg/ml) for 2 h at 37°C. The bactericidal activity was calculated on the basis of the number of cfu recovered after exposure to MIG/CXCL9 and after incubation in buffer alone (set as 100% survival). The mean values of at least three independent experiments are shown.

B. Electron micrographs of *S. pneumoniae* (TIGR4) incubated in buffer alone (a) or in presence of MIG/CXCL9 (2.4 μg/ml) (b-e). Bacteria exposed to MIG/CXCL9 show disintegration and leakage of intracellular contents. Scale bar; 0.5 μm.

C. Pairwise sequence comparison between human and mouse MIG/CXCL9. The alignment was generated using ClustalW.

D. Ribbon representation of theoretical models of human (cyan) and mouse (pink) MIG/CXCL9. Both molecules contain putative anti-parallel β-sheets in the NH_2-terminal region followed by an amphipatic α-helix and an unordered tail COOOH-terminal regions

Figure 3: Synergistic induction of MIG/CXCL9 production by TNF-α and IFN-γ in murine bronchial epithelial cells *in vitro.*

Murine bronchial epithelial cells (MLE-12) were stimulated with TNF-α (10 ng/ml) or IFN-γ (10 ng/ml) alone or in combination for 24 h. Supernatant from cells stimulated with culture medium was used as a control. Supernatants were collected and the MIG/CXCL9 concentrations were quantified using ELISA. The data shown represent mean ±SEM from three separate experiments. Data were analyzed by Student *t*-test. *, P<.05; **, P<.01; ***, P<.005

Figure 4: MIG/CXCL9 is expressed in the airways during pneumococcal infection *in vivo*.

Wt mice were intranasally infected with TIGR4 strain. Proinflammatory cytokines and chemokines were measured in lung homogenates. Ten mice per time point were used. Three control mice (C) were infected with 20 μl of control medium (PBS).

A. IFN-γ (black bars), TNF-α (grey bars) and MIG/CXCL9 (white bars) expression in the lungs of wt mice. Left Y-axis represents the IFN-γ and TNF-α concentrations in the lungs expressed in pg/ml. Right Y-axis represents the MIG/CXCL9 concentrations in the lungs expressed in ng/ml. Data are presented as means and SEM and were analyzed by Student *t*-test. *, P<.05; **, P<.01; ***, P<.005.

B. Histology of the lung tissue of wt mice at 24 h pi after infectious challenge. Pictures of representative lung sections are shown (4x, 20x and 40x magnification). Expression of MIG/CXCL9 in the lung tissue was detected by immunohistochemistry using polyclonal goat antibodies against murine MIG/CXCL9 (CXCL9). The negative staining was performed using a goat isotype control (NEG). The sections were also stained with Hematoxylin-Eosin solution (HE). The histopathological examination shows a marked inflammatory reaction with extensive recruitment of leukocytes, local bleeding, and alveolar exudates in the lung tissue. Large organ areas are severely congested and collapsed with accumulation of amorphic material from desquamation of the respiratory epithelium in the bronchi leading to airway obstruction. Immunohistochemistry staining shows local production of MIG/CXCL9 in the airways at 24h pi by granulocytes, endothelial an epithelial cells.

Figure 5: MIG/CXCL9 expression is dependent on the MyD88-signalling.

Wt, TLR4 KO, TLR9 KO and MyD88 KO mice were intranasally infected with a high infectious dose (10^7 cfu) of TIGR4. Proinflammatory cytokines and chemokines were

measured in lung homogenates 24 h pi. Data are presented as means and SEM and were analyzed by Student *t*-test. *, P<.05; **, P<.01; ***, P<.005.

A. IL-12 (black bars) and IFN-γ (white bars) concentrations in the lung tissue of wt (n=5) and MyD88 KO (n=5). Control mice (n=3) were infected with 20 μl of control medium (PBS).
B. MIG/CXCL9 expression in the lung tissue of wt (n=17) and TLR4 (n=9); TLR9 (n=16); MyD88 (n=9) KO mice. Control mice (n=3) were infected with 20 μl of control medium (PBS).

Figure 6: MIG/CXCL9 deficient mice are not more susceptible to streptococcal infections

Airway infection caused by *Streptococcus pneumoniae* in MIG/CXCL9 KO mice compared with wt mice. Survival of wt (*n*=10-15) and MIG/CXCL9 KO (*n*=10-15) mice after low (LD) and high (HD) infectious dose. The survival was analyzed by Kaplan-Meier log rank test.

Fig. 1

A

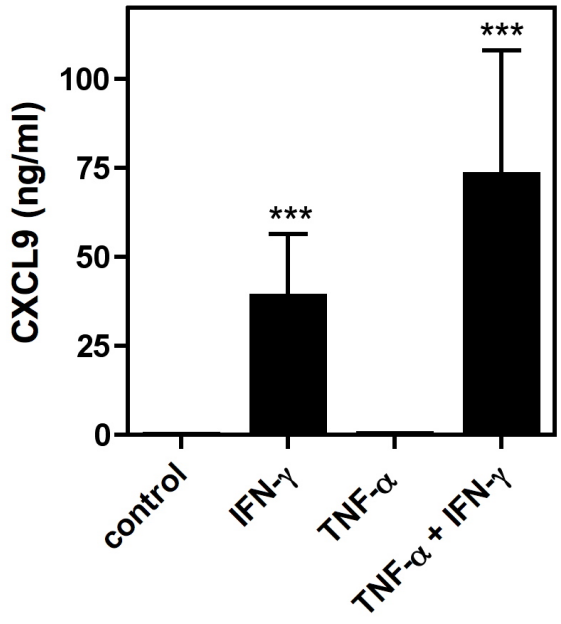
CXCL9 (ng/ml)
100
75
50
25
0
***
***
control
IFN-γ
TNF-α
TNF-α + IFN-γ

B

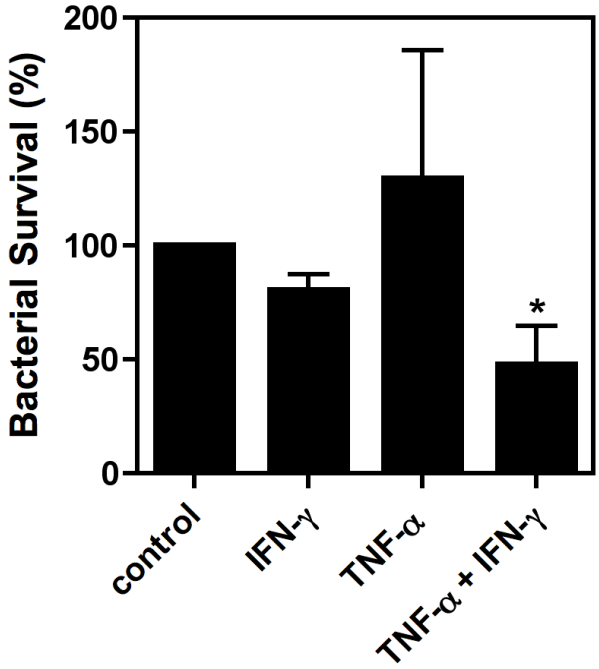
Bacterial Survival (%)
200
150
100
50
0
*
control
IFN-γ
TNF-α
TNF-α + IFN-γ

Fig. 2

A

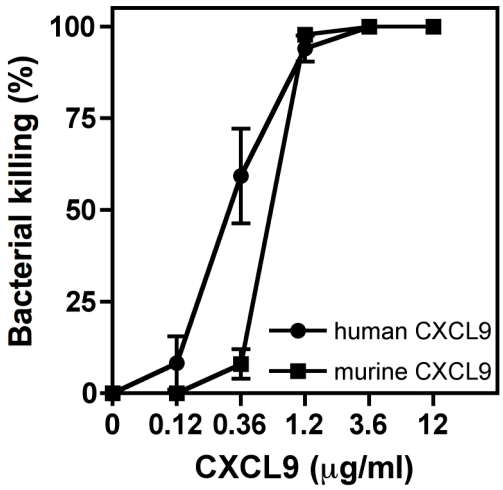
Bacterial killing (%)
100
75
50
25
0
0
0.12
0.36
1.2
3.6
12
CXCL9 (μg/ml)
human CXCL9
murine CXCL9

B

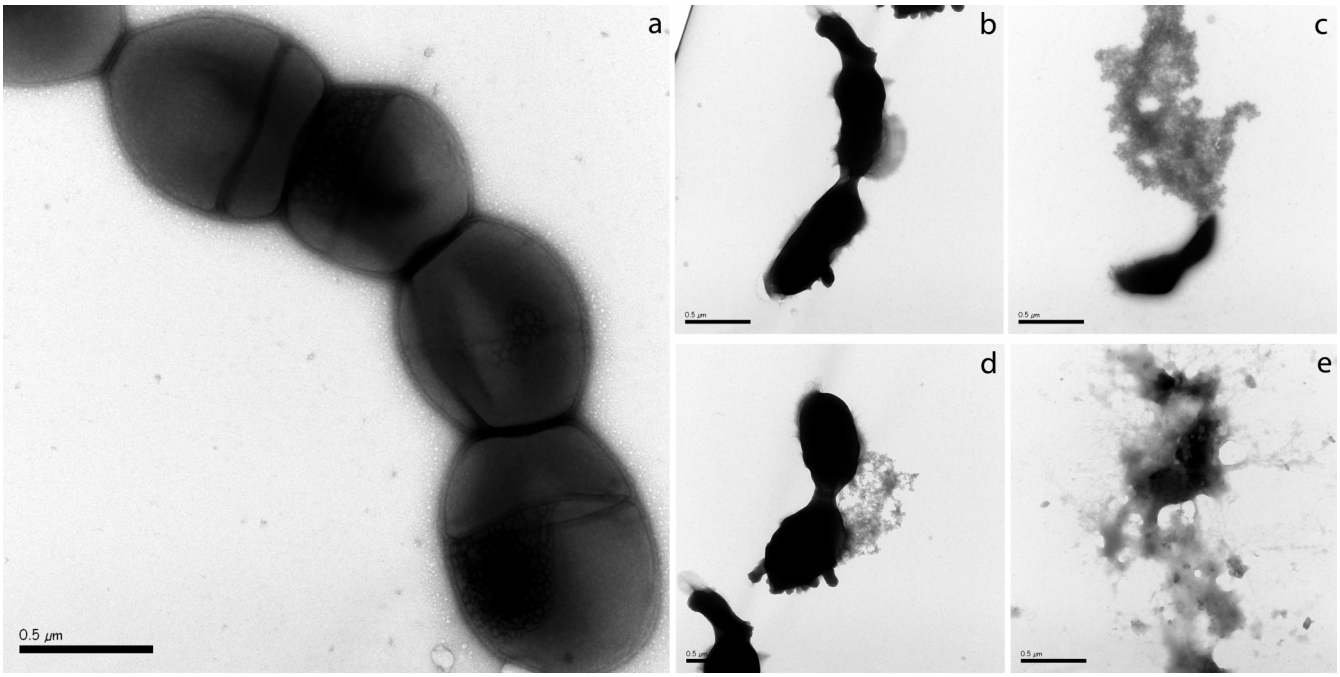
a
b
c
d
e
0.5 μm

C

```
                10         20         30         40         50         60         70
           ....|....| ....|....| ....|....| ....|....| ....|....| ....|....| ....|....|
CXCL9_MOUSE -MKSAVLFLL GIIFLEQCGV RGTLVIRNAR CSCISTSRGT IHYKSLKDLK QFAPSPNCNK TEIIATLKNG
CXCL9_HUMAN MKKSGVLFLL GIILLVLIGV QGTPVVRKGR CSCISTNQGT IHLQSLKDLK QFAPSPSCEK IEIIATLKNG
Clustal       **.***** ***:*   ** :** *:*:.* ******.:** ** :****** ******.*:*  *********

                80         90         100        110        120
           ....|....| ....|....| ....|....| ....|....| ....|....| ....|..
CXCL9_MOUSE DQTCLDPDSA NVKKLMKEWE KKINQKKKQK RGKKHQKNMK NRKPKTPQSR RRSRKTT
CXCL9_HUMAN VQTCLNPDSA DVKELIKKWE KQVSQKKKQK NGKKHQK-KK VLKVRKSQ-R SRQKKTT
Clustal      ****:**** :**:*:*:** *::.****** .******  *   * :..* *  *.:***
```

D

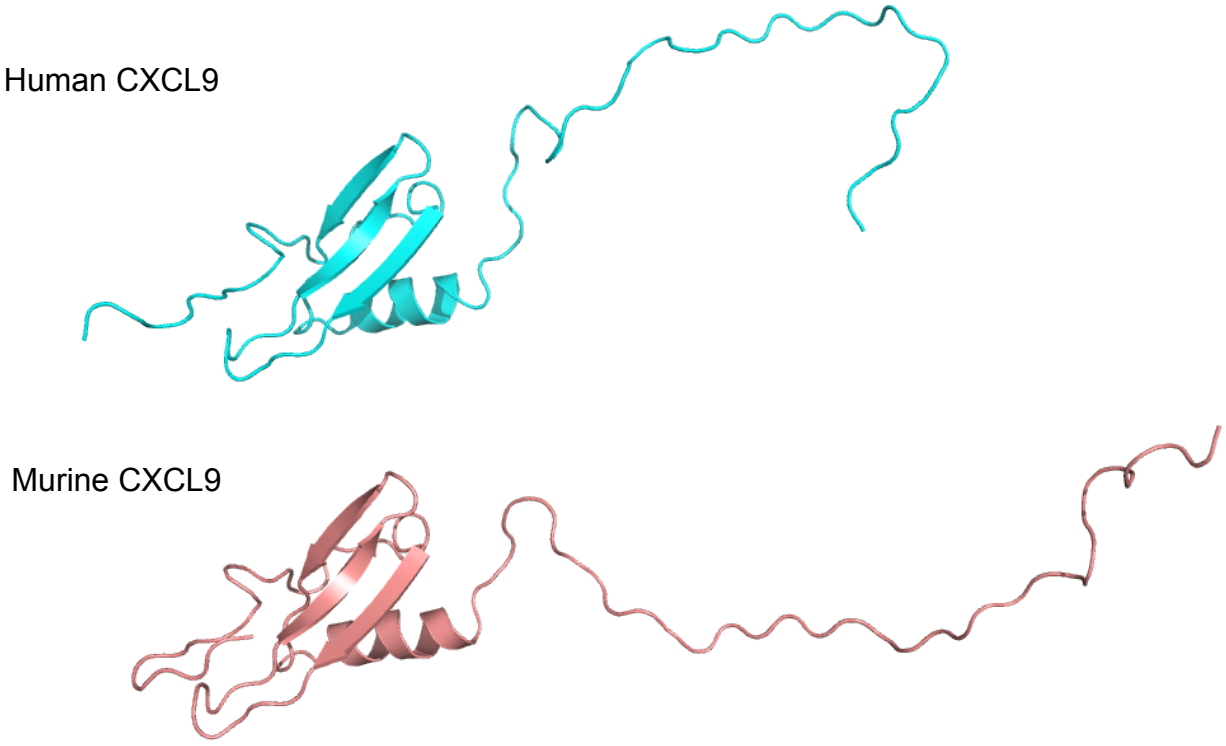

Fig. 3

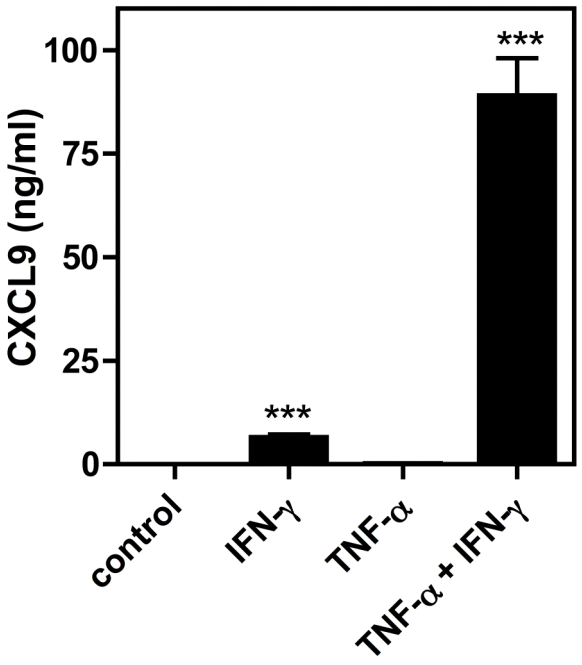

Fig. 4

A

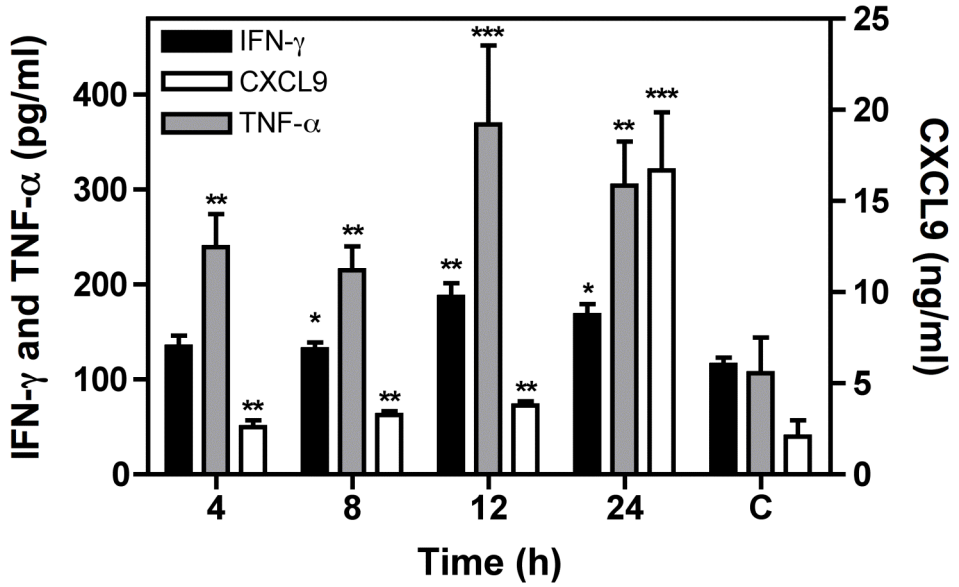
IFN-γ
CXCL9
TNF-α
IFN-γ and TNF-α (pg/ml)
CXCL9 (ng/ml)
0
100
200
300
400
0
5
10
15
20
25
4
8
12
24
C
Time (h)

B

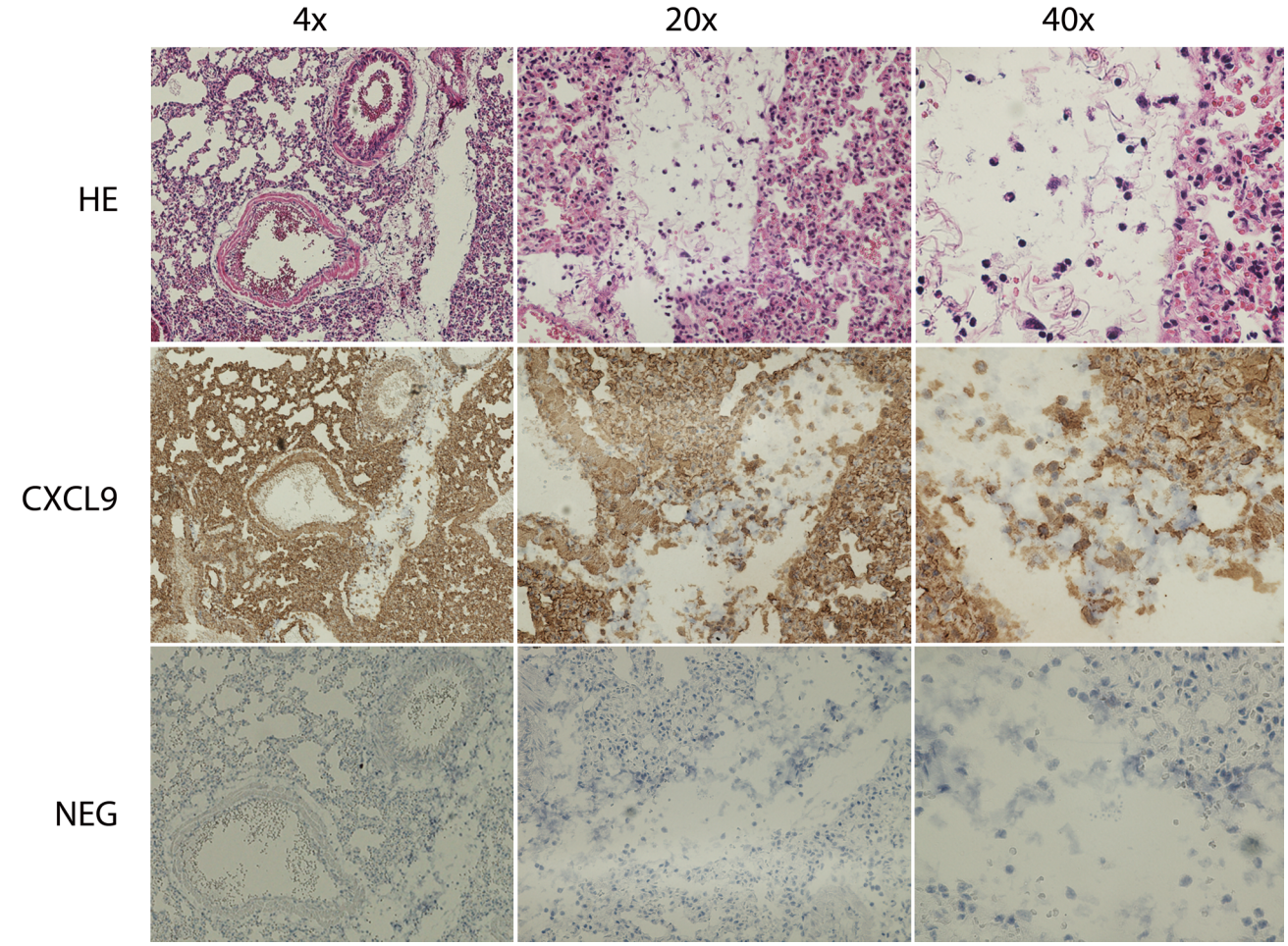
4x
20x
40x
HE
CXCL9
NEG

Fig. 5

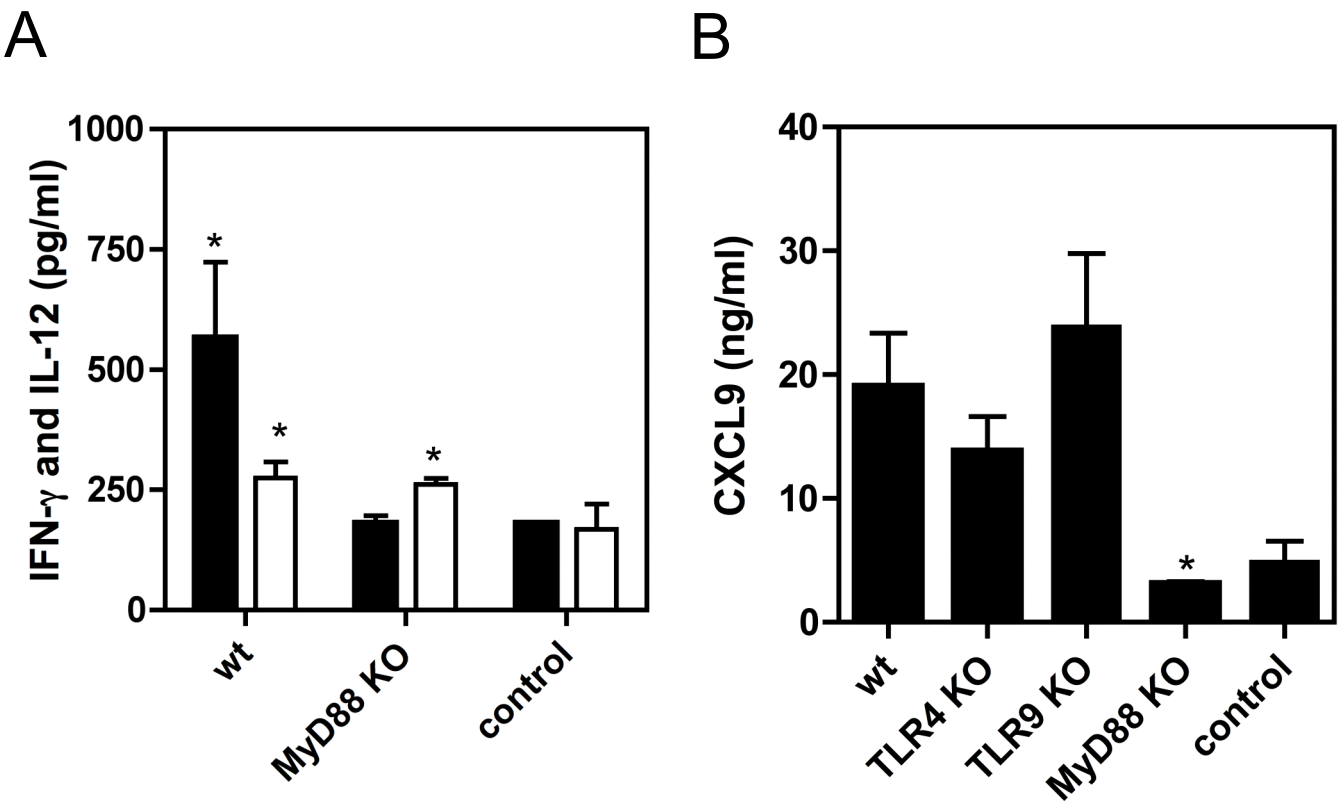
A
B
IFN-γ and IL-12 (pg/ml)
1000
750
500
250
0
*
*
*
wt
MyD88 KO
control
CXCL9 (ng/ml)
40
30
20
10
0
*
wt
TLR4 KO
TLR9 KO
MyD88 KO
control

Fig. 6

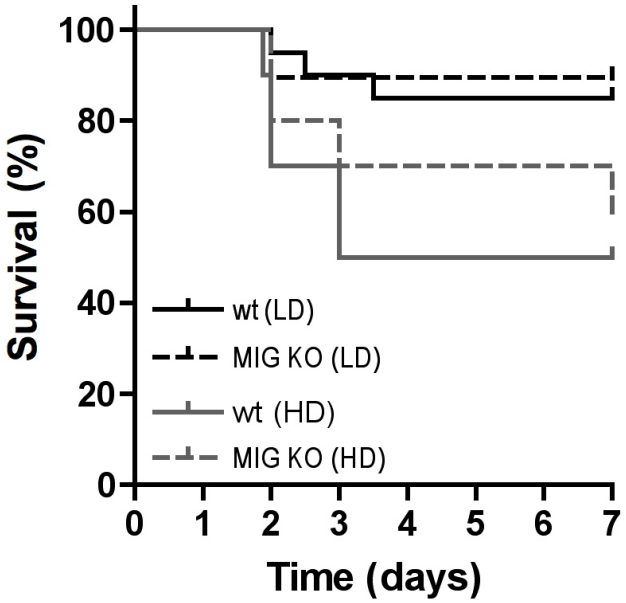
100
80
60
40
20
0
Survival (%)
wt (LD)
MIG KO (LD)
wt (HD)
MIG KO (HD)
0
1
2
3
4
5
6
7
Time (days)